A THEORETICAL ANALYSIS OF A YAW DAMPER SERVOMECHANISM

BY

LAURENCE B. RICHARDSON JR.

PRINCETON UNIVERSITY

AERONAUTICAL ENGINEERING LABORATORY

REPORT NO. 172

THESIS
R39

A THEORETICAL ANALYSIS OF THE APPLICATION OF A YAW DAMPER SERVOMECHANISM TO IMPROVE LATERAL OSCILLATORY STABILITY

by

Laurence B. Richardson Jr.
Lieutenant
United States Navy

Submitted in partial fulfillment of the requirements for the degree of Master of Science in Engineering from Princeton University, 1951.

SUMMARY

The purpose of this analysis is to investigate the use of an automatic control to damp undesirable lateral oscillations. The type of control under consideration is a yaw damper servomechanism with rudder control applied in proportion to yawing velocity. The effect of angle of attack and gyro axis angle on components of roll and yaw picked up is developed, and the optimum angle of tilt of the gyro axis is selected. The problems of maintaining equal effectiveness of the control through the speed range, eliminating yaw compensation during steady turning or rolling maneuvers, critical time lag, and prevention of feedback to the pilot's controls are considered.

The airplane used for the analysis is an operational jet fighter of high performance which has been reported to have a "snaking," or "Dutch Roll" problem. The flight conditions investigated are cruising at 35,000 feet, 50% normal rated power at 10,000 feet, and power approach at sea level. Calculations in these configurations predict that the aircraft has an unsatisfactory "Dutch Rolling" tendency, probably in all flight conditions. Installation of the proposed damper system will enable the airplane to satisfactorily meet the lateral-directional oscillation requirements. In addition, the stabilizer will cause the aircraft to be spirally stable, and will have the effect of gearing the rudder to the ailerons for improved entry into rolling or turning maneuvers.

SYMBOLS AND COEFFICIENTS

α angle of attack measured from the flight path to the airplane reference axis, degrees

θ angle between the reference axis and the horizontal axis, positive when the reference axis is above the horizontal axis, degrees

γ angle of the flight path to the horizontal, positive in a climb, degrees

η angle of attack of the principal longitudinal axis of the airplane, positive when the principal axis is above the flight path at the nose, degrees

ε angle between the reference axis and the principal axis, positive when the reference axis is above the principal axis, degrees

ν angle between the gyro spin axis and the reference axis, positive when the reference axis is above the gyro axis, degrees

ξ angle between the flight path and the gyro axis, positive when the gyro axis is above the flight path, degrees

Ψ angle of aximuth, radians

ϕ angle of bank, radians

β angle of sideslip, radians (v/V)

v sideslip velocity along the Y axis, feet per second

V true airspeed, feet per second

ρ mass density of air, slugs per cubic feet

σ density ratio, ρ/ρ_o

q dynamic pressure, pounds per square foot ($1/2\ \rho V^2$)

W weight of airplane in pounds

m mass of airplane in slugs, W/g

g acceleration of gravity, feet per second per second

μ relative density factor, $m/\rho Sb$

m_o factor for dimensionalization, $2b\ \mu/V$

C_L trim lift coefficient, $W \cos \gamma / qS$

M mach number

b wing span in feet

ℓ_t distance from the center of gravity of the airplane to the center of pressure of the fin, feet

S wing area in square feet

S_D control surface area for yaw damper in square feet

S_{vt} vertical tail area in square feet

S_r rudder area in square feet

h distance from the longitudinal body axis to the center of pressure of the vertical control surface

D the operator, d/dt

P period of oscillation in seconds

$T_{1/2}$ time for amplitude of oscillation to damp to one-half of its original amplitude in seconds

$C_{1/2}$ cycles for the amplitude of oscillation to damp to one-half of its original amplitude

K control gearing, or gain, $\left|\frac{\partial \delta_r}{\partial \psi}\right|$

K_c amplitude ratio of damper, $1/K$ or $\left|\dot{\psi}/\delta_r\right|_{\text{Damper}}$

K_A airplane amplitude, $\left|\dot{\psi}/\delta_r\right|$

I_{x_o} moment of inertia about the principal longitudinal axis in slug feet squared

I_{z_o} moment of inertia about the principal normal axis in slug feet squared

I'_x moment of inertia coefficient about the principal longitudinal axis. I_{x_o}/qSb

I_x moment of inertia coefficient about the flight-path axis, $(I'_x \cos^2\eta + I'_z \sin^2\eta)$

I_z moment of inertia coefficient about axis normal to flight path, $(I'_z \cos^2\eta + I'_x \sin^2\eta)$

I'_z moment of inertia coefficient about the principal normal axis. I_{z_o}/qSb

I_{xz} product of inertia coefficient with respect to flight path axis and axis normal to flight path, $-(I'_z - I'_x)\sin\eta\cos\eta$

C_l rolling moment coefficient $(\frac{\text{rolling moment}}{qSb})$

C_n yawing moment coefficient $(\frac{\text{yawing moment}}{qSb})$

C_Y side force coefficient $(\frac{\text{lateral force}}{qS})$

$r, \dot{\psi}$ angular yawing velocity in radians per second

$p, \dot{\phi}$ angular rolling velocity in radians per second

$$C_{l_\beta} = \frac{dC_l}{d\beta} \qquad C_{n_\beta} = \frac{dC_n}{d\beta}$$

$$C_{l_r} = \frac{dC_l}{d(\frac{rb}{2V})} \qquad C_{n_r} = \frac{dC_n}{d(\frac{rb}{2V})}$$

$$C_{l_p} = \frac{dC_l}{d(\frac{pb}{2V})} \qquad C_{n_p} = \frac{dC_n}{d(\frac{pb}{2V})}$$

$$C_{l_{\delta_r}} = \frac{dC_l}{d\delta_r} \qquad C_{n_{\delta_r}} = \frac{dC_n}{d\delta_r}$$

$$C_{l_{\dot{\psi}}} = C_{l_r}\frac{b}{2V} \qquad C_{n_{\dot{\psi}}} = C_{n_r}\frac{b}{2V}$$

$$C_{l_{\dot{\phi}}} = C_{l_p}\frac{b}{2V} \qquad C_{n_{\dot{\phi}}} = C_{n_p}\frac{b}{2V}$$

$$C_{Y_\beta} = \frac{dC_Y}{d\beta} \qquad C_{Y_r} = \frac{dC_Y}{d\frac{rb}{2V}}$$

$$C_{Y_{\delta_r}} = \frac{dC_Y}{d\delta_r} \qquad C_{Y_p} = \frac{dC_Y}{d\frac{pb}{2V}}$$

The standard NACA conventions in regard to directions of axes, angles, control deflections, forces, moments, and linear and angular motions are used. Where dotted quantities are written, they indicate time derivatives, ie, $\ddot{\psi} = \frac{d^2\psi}{dt^2}$.

INTRODUCTION

The purpose of this report is to conduct a theoretical investigation into the use of a yaw damper servomechanism to improve the lateral dynamics of an operational high speed jet fighter. Calculations, flight tests, and pilots reports indicate that this aircraft does not satisfactorily meet the requirements of NAVAER SR-119B, "Specifications For Flying Qualities of Piloted Airplanes," in regard to the damping of the lateral-directional oscillation, controls free or fixed.

High performance requirements of present day aircraft and those of the immediate future are leading to designs in which lateral dynamic flight stability is becoming a serious problem. "Dutch roll" at low airspeeds, particularly on landing approaches, is annoying, fatiguing, and dangerous to the pilot. It makes instrument approaches particularly difficult. The present day trend toward sweepback and low aspect ratio causes high effective dihedral at low apeeds and also reduces the damping in roll and increases the adverse yaw due to roll. These factors combine to contribute to unsatisfactory lateral dynamics. "Snaking," the control free lateral dynamic oscillation, compromises the effectiveness of the aircraft in carrying out its mission as a gunnery or bombing platform. Satisfactory solutions to the problems of "Dutch roll," and "snaking" will not only improve the flying qualities, but will give the designers more freedom in still higher performance designs.

Considerable work is being done by various investigators on the causes of these unsatisfactory lateral oscillations. Aerodynamic balance of the rudder is a probable major cause. Reference 2 traced the poor damping qualities

of its test airplane (Navy AD) to the rudder hinge moment characteristics. Reference 3 points out as a possible cause the effect of fuel sloshing on airplane dynamics. Non-linearity of the directional stability and damping-in-yaw derivatives is shown to be a possible cause in reference 4. Random separation phenomena such as flow at the tail-fuselage juncture and at the tail pipe have been demonstrated to have important effects. Reference 5 shows that positive inclination of the principal axis can have considerable stabilizing influence. Here wing incidence has an important effect. It has been demonstrated theoretically that atmospheric turbulence can initiate and maintain lateral oscillations.

The designer is faced with an imposing problem in selecting the proper hinge moment parameters, which will satisfy control force and other requirements, and still not invite snaking. Reference 2 discusses this problem. Irreversible power-boosted control systems offer a promising solution. In any case, it has become apparent that some means must be found to augment aerodynamic damping. The increment needed is considerably in excess of the amount that can be provided by an increase of vertical tail area or tail length. It can be shown that the tail volume coefficients should be determined by the requirements for static sideslip stability, unsymmetrical power, and stalling qualities, and that other methods should be sought to add to aerodynamic damping.

Although hinge moment parameters combined with friction and slack in the control systems explain conventional rudder snaking in many cases, others are on record in which the rudder has been locked or observed not to move. Usually the calculated and tested control fixed periods and times to damp

agree quite well. The case under consideration in this paper is one of the latter group. The manufacturer felt that the lateral oscillations were traceable to non-linearities in the derivatives and to separation effects. It was originally thought that fuel sloshing was a contributory cause, but baffling was installed and found to have no noticeable effect. In their tests they confirmed the effectiveness of a "de-boost" tab, as reported in reference 2. Since there are no known aerodynamic fixes for the poor damping in the rudder fixed condition, an automatic stabilization device provides the most promising solution.

It is the purpose of this analysis to consider the effect of using a servo stabilizing control, and to select an optimum setting of gain and spin axis angle for this application. Two systems are already commercially developed (by Minneapolis-Honeywell and Boeing for the XB-47, reference 8, and by Lear for use in conjunction with the F-5 autopilot, reference 6). The theoretical investigation is here conducted with the use of one of these types of servomechanisms in mind.

Reference 7 considers stabilizing devices sensitive to various quantities and concludes that the only one which has the capability of satisfactorily meeting the requirements of reference 1 is an autopilot which supplies rudder control proportional yawing velocity. This is the type of yaw damper referred to above. This reference and the above mentioned systems neglect the problem of the tilt of the gyro axis. The gyro, which is the rate of yaw sensing device, will pick up components of roll as well as yaw, and at only one angle of attack will be a pure yaw sensing instrument as is customarily assumed. This fact can be used advantageously to effectively gear the rudder

to the ailerons by making the yawing moment due to roll positive. This eliminates adverse yaw upon entry into turns and rolling maneuvers. A stabilizing device can be designed then that will improve the damping in yaw to meet the lateral oscillation requirements, making the aircraft spirally stable at the same time, and also improve the response to the rolling control. The problem of maintaining equal effectiveness of this control with variations in speed is also discussed in this analysis.

DESCRIPTION OF THE AIRPLANE AND THE DAMPER SYSTEM

The airplane under consideration is a single seat, midwing, high performance jet propelled fighter with a conventional control system. It has a two piece rudder actuated by cables from the rudder pedals, not power boosted. The physical characteristics, dimensions, and stability derivatives were supplied by the manufacturer and checked with independent wind tunnel data or methods of calculation as specified by the NACA.

The damper system to be applied in this case would be known as a force type as opposed to a power-boosted type. This means that the servo drive has to have an output of the same order of magnitude as a human pilot's control effort. In the other case, the servo drive can operate into an artificial feel system, boost, or irreversible control power control system. Of course, the time lag of this force type system is not increased by the inclusion of the time lag inherent in hydraulic rudder boost systems. Considerable range in power size is available to meet varying requirements. Time lags for a force type system can be reduced to less than one tenth of a second.

The proposed damper system is comprised of three principal parts. (1) A rate gyro, a single degree of freedom gyro mounted with its spin axis in the XZ plane of the aircraft at some angle to the body reference axis. It is constrained by a spring control whose restraint is caused to vary to compensate for speed changes. The gyro produces a precession displacement and a corresponding electrical signal proportional to the angular rotation of the aircraft in space. (2) A controller-amplifier section, which receives the rate signals from the rate gyro, amplifies this signal and imparts phase lead. It contains a derivative network which will not pass steady signals

from the rate gyro. This network prevents the damper from opposing the pilot in a steady state maneuver such as a turn or roll. Any transient disturbances in the steady state maneuver will be damped out, however, and the beneficial damper contribution upon entry into these maneuvers passes. The gain and the phase lead are adjustable to obtain the optimum settings for particular applications. The compensating spring restraint feature could be included in this unit instead of at the gyro. A typical unit would also house the rate gyro in its chassis. (3) The servo drive supplies the power to move the rudder upon signal from the amplifier-controller. If used in an irreversible application (which it is not in this case) the feedback from the load, or position follow-up would not be required since the artificial feel spring systems will recenter the load when the signal vanishes.

The total weight of this system could be kept to within fifteen pounds, and the space required to less than one third of a cubic foot. The gyro should be located near the center of gravity so as to escape the effects of body bending. In this case body bending should be a negligible. This problem is treated in reference 8.

It is appropriate that the distinction between an autopilot and a stabilizing device should be mentioned. The autopilot has authority over the aircraft, presumably by the choice of the pilot. He may overpower it or control it through autopilot control settings, but the autopilot has direct control of the aircraft. A stabilizing device, such as the proposed yaw damper, operates in conjunction with the pilot; the pilot, however, has control and is superimposing his control motions over the damper. The damper can be thought of in the same sense as the vertical tail in that it is a part

of the aircraft which is in continual operation contributing stability. It is the opinion of the author that it should be an absolute requirement that a stabilizer shall have no feedback to the control system of the pilot; the pilot should not be conscious of the damper's operation except that he feels that the flying qualities are improved, and that he is able to fly a more highly damped and smoother path. This isolation can be easily accomplished in an irreversible control system. In the application under consideration it poses a difficult problem that can probably be best solved by dividing the two piece rudder between the pilot and the damper. That is, using a control surface for the damper alone. No solution in which the pilot can feel the damper in operation through the rudder pedals should be considered satisfactory.

LATERAL DYNAMIC CHARACTERISTICS

The first step in the problem is to determine what the calculated lateral-directional oscillation characteristics of the aircraft are.

Three configurations of the aircraft have been considered.

I. The maximum cruise configuration, at 35,000 feet, clean, at a Mach number of .68.

II. The 50% Normal Rated Power configuration at 10,000 feet, clean, at a Mach number of .32.

III. The Power Approach condition with flaps and gear down and with power for level flight at a reasonable approach speed.

These three conditions give a sufficient range of altitude and speed to reasonably judge the lateral dynamics of the aircraft with and without a damper system. Configuration II was selected because pilots reports have indicated that at that particular altitude, at Mach numbers below .6, the Dutch Roll or snaking has been particularly noticeable. Conditions I and III represent the extreme opposite ends of the speed and altitude range in configurations of operational interest.

The equations of motion as presented in reference 9 have been used, with the exception that the effects of the product of inertia have been included only in condition I. In this condition η is negative. In the other two conditions η is positive and it is conservative to neglect the product of inertia. For this particular aircraft the product of inertia was found to have little effect. These calculations are reviewed in the section on calculations. The data is presented in Table II and plotted in figure 2.

All the points lie in the unsatisfactory region. Flight tests have

shown good correlation with these points. The calculations are control fixed, indicating an unsatisfactory Dutch Roll characteristic. The boundary between the satisfactory and unsatisfactory regions of figure 1 of reference 1 is currently under investigation. The calculated points show the aircraft to be in a region which has been called tolerable, meaning tiring or unpleasant, but not necessarily dangerous. The calculations show that a condition exists which would certainly be annoying and detrimental to the carrying out of the airplane's mission.

Whether this condition is of sufficient severity to warrant a change or modification in already operational units is doubtful. That is a question of opinion of the pilots operating the airplane. All indications are that future designs are going to need automatic stabilization; analyses of this type will be called for. Applications to longitudinal motions are also in use. Future airplanes may well use automatic stabilization both laterally and longitudinally with the pilot imposing his control efforts over the automatic controls.

CONTRIBUTION OF THE YAW DAMPER

Referring to figure 1b the relation between the body reference axis, the gyro spin axis, and the wind or stability axis is shown. Subscripts R (reference), G (gyro), and V (stability) are used in the following development.

For simplification the time lag of the yaw damper system is first assumed to be zero. It will be later shown that the critical time lag of the aircraft-stabilizer system is considerably higher than the time lag of any mechanism under consideration.

The equations of motion are written with respect to the wind or stability axes. The derivatives contributed by the damper must therefore be related to the V axis for inclusion in the equations. The rudder, however, introduces yawing and rolling moments about the reference or body axis R. Also the yawing and rolling moments so introduced are proportional to the rate of yaw as measured with respect to the gyro axis G.

Then the development of the contributions of the damper is as follows:

$$K = \left|\frac{d\delta_r}{d\Psi}\right|_G \text{ rad/rad/sec} \quad \text{control gearing or gain.}$$

$$(C_n)_B = C_{n_{\delta_r}} \delta_r = C_{n_{\delta_r}} K \dot{\Psi}_G$$

$$(C_\ell)_B = C_{\ell_{\delta_r}} \delta_r = C_{\ell_{\delta_r}} K \dot{\Psi}_G$$

but

$$\dot{\Psi}_G = \dot{\Psi}_V \cos\xi + \dot{\phi}_V \sin\xi$$

and

$$C_n = (C_n)_V = (C_n)_B \cos\alpha + (C_\ell)_B \sin\alpha$$

$$C_\ell = (C_\ell)_V = (C_\ell)_B \cos\alpha + (C_n)_B \sin\alpha$$

substituting into the above equations,

$$C_n = K C_{n_{\delta_r}} [\dot{\psi}_V \cos\xi + \dot{\phi}_V \sin\xi] \cos\alpha$$

$$+K C_{\ell_{\delta_r}} [\dot{\psi}_V \cos\xi + \dot{\phi}_V \sin\xi] \sin\alpha$$

$$C_\ell = K C_{\ell_{\delta_r}} [\dot{\psi}_V \cos\xi + \dot{\phi}_V \sin\xi] \cos\alpha$$

$$+K C_{n_{\delta_r}} [\dot{\psi}_V \cos\xi + \dot{\phi}_V \sin\xi] \sin\alpha$$

These expressions can be seen to have the form of total derivatives, where

$$\Delta C_n = \frac{dC_n}{d\dot{\psi}} \Delta\dot{\psi} + \frac{dC_n}{d\dot{\phi}} \Delta\dot{\phi}$$

$$\Delta C_\ell = \frac{dC_\ell}{d\dot{\psi}} \Delta\dot{\psi} + \frac{dC_\ell}{d\dot{\phi}} \Delta\dot{\phi}$$

therefore

$$\Delta C_{n_{\dot{\psi}}} = K \cos\xi \; [C_{n_{\delta_r}} + C_{\ell_{\delta_r}} \alpha]$$

$$\Delta C_{n_{\dot{\phi}}} = K \sin\xi \; [C_{n_{\delta_r}} + C_{\ell_{\delta_r}} \alpha]$$

$$\Delta C_{\ell_{\dot{\psi}}} = K \cos\xi \; [C_{\ell_{\delta_r}} + C_{n_{\delta_r}} \alpha]$$

$$\Delta C_{\ell_{\dot{\phi}}} = K \sin\xi \; [C_{\ell_{\delta_r}} + C_{n_{\delta_r}} \alpha]$$

since

$$C_{n_{\dot{\psi}}} = C_{n_{\frac{rb}{2V}}} \frac{b}{2V} = C_{n_r} \frac{b}{2V} \quad \text{etc.}$$

$$\Delta C_{n_r} = \frac{2V}{b} K \cos \xi_r \; C_{n_{\delta_r}}$$

$$\Delta C_{n_p} = \frac{2V}{b} K \sin \xi_r \; C_{n_{\delta_r}}$$

neglecting the product $\alpha C_{\ell_{\delta_r}}$, which is small compared to $C_{n_{\delta_r}}$.

The damper contributions are seen to be directly proportional to true airspeed. The rudder power also is seen to vary with altitude from Table II.

The rudder power coefficient has a negative sign, and the rolling coefficient due to rudder deflection has a positive sign. It can be seen, therefore that if ξ_r has a negative sign the increments $\Delta C_{n_{\dot{\phi}}}$ and $\Delta C_{\ell_{\dot{\psi}}}$ will be positive, and the increments $\Delta C_{n_{\dot{\psi}}}$ and $\Delta C_{\ell_{\dot{\phi}}}$ negative. These are the desirable signs for these contributions by the damper. It is therefore concluded that the gyro axis should be so set that it is always below the stability axis, (ξ_r a negative angle) as shown in figure 1c.

The increments $\Delta C_{\ell_{\dot{\phi}}}$ and $\Delta C_{\ell_{\dot{\psi}}}$ have little effect on the lateral dynamic calculations, and sum $[C_{\ell_{\delta_r}} + C_{n_{\delta_r}} \alpha]$ is considerably less than $[C_{n_{\delta_r}} + C_{\ell_{\delta_r}} \alpha]$; for these reasons the conservative assumption is made in further calculations that only $\Delta C_{n_{\dot{\psi}}}$ and $\Delta C_{n_{\dot{\phi}}}$ are supplied by the yaw damper.

The increments added by the yaw damper are then assumed to be

$$\Delta C_{n_{\dot{\psi}}} = K \cos \xi \; C_{n_{\delta_r}}$$

$$\Delta C_{n_{\dot{\phi}}} = K \sin \xi \; C_{n_{\delta_r}}$$

The optimum settings of K and $\xi = f(\alpha, D)$ are discussed in a later section.

Reference 10 treats the effect of C_{n_p} ($\frac{2V}{b} C_{n_{\dot{\phi}}}$) on lateral dynamic stability. Making $C_{n_{\dot{\phi}}}$ positive was shown to have a beneficial effect in shifting the points on a plot such as figure 4 to the satisfactory area. As K and $-\xi$ are increased, the positive increment of $C_{n_{\dot{\phi}}}$ lengthens the period at substantially the same time to damp to one-half amplitude, improving the cycles to damp to one-half amplitude. This increment in $+C_{n_p}$ must be limited, however, since too great an amount leads to a long period unstable oscillation of the roots that were identified as the rolling convergence and the spiral mode. These roots first become a long period stable oscillation and then as $C_{n_{\dot{\phi}}}$ is further increased the oscillation becomes unstable. This shows that the product $VK \sin \xi$ must be limited so as to be satisfactory in configurations as contrasting as I and III.

The reasons for seeking $+C_{n_{\dot{\phi}}}$ contributions from the damper are to assist in correcting the Dutch Roll oscillations and to oppose the adverse yaw introduced by the ailerons and the normal negative derivative (adverse) of yaw due to roll. By overcoming the adverse yaw in this manner, entry into rolls and turning flight can be considerably improved. This benefit can only be enjoyed on the entry into these maneuvers, since the steady yawing velocity signal will be intentionally blocked to keep the yaw damper from opposing a steady turn initiated by the pilot.

$C_{n_{\dot{\phi}}}$ is seen to have its greatest influence in the b_1 term of the stability quartic. As this derivative becomes more positive it drives b_1 to zero. As this occurs the rolling and spiral modes first become a stable oscillation, and finally a long period unstable oscillation. The limiting value of $-\frac{b}{\xi}$ for the fixed K was then calculated by setting b_1 to zero, keeping all derivatives except $C_{n_{\dot{\phi}}}$ and $C_{n_{\dot{\psi}}}$ the same, and introducing these as $f(\frac{b}{\xi})$. The limiting ν determined in condition I is shown in figure 3. Since α varies over a small known range, and $\frac{\psi}{\xi} = \alpha - \nu$, it is possible to estimate the range of effective $\frac{b}{\xi}$. See figures 1c, 3.

ΔC_{n_r} and ΔC_{n_p}, the non-dimensional forms of the damper contributions, were seen to vary with speed. Therefore in order to maintain equal effectiveness of the stabilizing control throughout the speed range, K must be made to vary inversely with speed. One convenient way to do this is to apply the inverse of $q^{1/2}$ to the spring restraint of the gyro, thereby modifying the electrical signal from it. The V's will cancel, but a varying factor of $\sigma^{-1/2}$ remains that will have to be calibrated out as well as possible. A close approximation to the desirable variations in K with the three conditions is shown in Table III (K to make $C_{1/2} = .5$). Comparing these values with those shown in Table II (calculated by using a $q^{-1/2}$ variation) it is seen that the contributions tend to be too large at altitude. Figures 2, 3, and 4 confirm this. Applying dynamic pressure from a pitot source seems to be the most convenient way of compensating, however. A non-linear spring and bellows with a pitot tube source such as are used in artificial feel systems would probably be the best solution. This penalty in gadgetry must be paid to realize the benefits of the positive yaw due to roll introduced by the damper. Positive C_{n_p} must be limited, and the goal should be similar performance at all altitudes and speeds.

SETTING GYRO AXIS ANGLE AND GAIN

The question of just how damped a motion the pilot would like to have is still under considerable discussion. There is no question that in a system of this sort it would be possible to add enough damping with a stabilizer to the aerodynamic damping to critically damp all lateral oscillations. However, the standards for the performance and stability of the aircraft-stabilizer servomechanism are not as yet established. See references 11 and 12.

This analysis was made on the assumption that the gain should be the minimum required to bring the cycles to one-half amplitude to one half. There is evidence to show that the motion will then appear critically damped to the pilot. Reference 8.

A Routh's discriminate investigation using K and $\frac{b}{\xi}$ as variables is possible, but exceedingly tedious. Determination of the optimum values of these variables by a plot of $C_{1/2}$ vs D with K as a parameter is shown in figure 3. This approach is relatively easy and equally informative.

Referring to figure 3, curves for $K = 1$ and $K = 2$ in condition III are shown. The higher value of K does not give sufficiently better results to warrant the higher gain settings. It is in this condition (sea level at approximately 1.20 V_{stall}) that the basic value of the gain, or control gearing, is established. At higher speeds (or q's) the gain is reduced as already explained.

Selecting the basic value of $K = 1$ in condition III, the effective value in condition I becomes .5, in condition II, .817. The curve for condition I for this effective K is shown up to the limiting value of D ,

determined as discussed in the previous section. In this particular case there is no limit to the gyro angle in condition III. In other words with gains below 2, too much $+C_{n_p}$ cannot be introduced. The effect of holding K constant and inclining the gyro axis to the point that damper contribution is entirely ΔC_{n_p} is shown in figure 4. The points of $\S = 0$ and $\S = -90^\circ$ on each curve contrast the effects of stabilizers sensitive to pure yaw or pure roll.

Selecting a gyro angle of 30° and $K = 1$, the range of values of $C_{1/2}$ for a variation of angle of attack of fifteen degrees is shown. This setting of D and K is taken for further investigation since it is the maximum practical gyro angle at this K that will not introduce an unstable oscillation due to too much $+C_{n_p}$ in condition I. Some lower angle might prove more desirable from flight tests. This is a question of how much positive yaw due to roll is best for entry into rolls or turns. From figures 8, 9, and 10 it can be seen that the response to the aileron control is radically modified.

In general, a quick procedure for selecting gyro angle and gain is as follows:

(1) Using the single degree of freedom equation in yaw, a close estimate of the total amount of damping required to damp to any given $C_{1/2}$ is easily obtainable. From this, the amount of $\Delta C_{n_{\dot{\psi}}}$ that is to be added by the damper can be estimated. Knowing the rudder power, the approximate gain to get this increment of damping can be found.

(2) From the adverse yaw and yaw due to roll coefficients the total amount of $+\Delta C_{n_{\dot{\phi}}}$ desired can be estimated. Using the gain calculated above,

the required ξ to get the increment in $+C_{n_\phi}$ estimated above can be solved for, using the expression obtained under the damper contribution section. For the gyro angle, $\Box = \alpha - \xi$.

The compensating device on the gyro will keep these increments essentially constant with speed and altitude. To check to see if an instability has been introduced, select a high speed condition where the final ratio of $C_{n_{\dot\phi}}$ to $C_{n_{\dot\psi}}$ is high (usually at high altitude and speed) and calculate the b_1 term of the stability quartic.

Final checks using the three degree of freedom equations and involving a separate solution of the quartic for each point as was done in figure 3 can then be made for a critical configuration. The assumption of zero time lag will have to be kept in mind and later checked. At this point it probably would be desirable to begin flight testing the system for the final selection of these paramenters.

In order to prevent any feedback through the pilots rudder control system, the yaw damper for this application will probably have to have its own rudder area. The calculations in this report have been made on the assumption that the whole rudder was available for the yaw damper. This can be done when the movements of the rudder caused by the damper can be masked from the pilot through a boosted or artificial feel control system.

$$C_{n_{\delta_r}} = -C_{L_{\delta_r}} \frac{S_D \ell_t}{Sb}$$

and

$$C_{\ell_{\delta_r}} = C_{L_{\delta_r}} \frac{S_D h}{Sb} = -\frac{h}{\ell_t} C_{n_{\delta_r}}$$

The terms involving $C_{l_{\delta_r}}$ have been neglected in the development of the contribution of the yaw damper. Since

$$\Delta C_{n_{\dot{\psi}}} = K \cos \xi \; C_{n_{\delta_r}}$$

$$\Delta C_{n_{\dot{\phi}}} = K \sin \xi \; C_{n_{\delta_r}}$$

the same results can be obtained by keeping the product of $KC_{n_{\delta_r}}$ constant: or as the area S_D, for the damper, is reduced, the gain K is increased. Note that the vertical location of the area for the damper is a negligible effect. The maximum practical value of K obtainable with this type of installation (probably 2 or 3) will limit the minimum size of the damper rudder area.

In summary, the optimum gyro angle is chosen as 30 degrees, and the optimum gain as 1 at sea level and approach speed. This setting has the following results:

(1) Moves the points shown in figure 2 from the unsatisfactory region to the satisfactory damping region where $C_{1/2}$ is less than .5.

(2) Adds a sufficient amount of $\Delta C_{n_{\dot{\psi}}}$ in each case to make the aircraft spirally stable in all conditions.

(3) Adds a $+C_{n_{\phi}}$ increment of an approximately constant value to all conditions, which is considerably larger than the total adverse yaw due to roll and the rolling control.

The beneficial effect of the additional damping is shown in the response data plotted in figures 5, 6, and 7. The improved response to the rolling control is shown in the response data plotted in figures 8, 9, and

10.

The effect of varying ν at a constant K for condition III is shown in figure 4.

Figure 3 shows the selected points in the three conditions, and a $C_{l/2}$ vs ν plot for constant K for conditions I and III including the range of angles of attack.

All calculations involving the contributions from the yaw damper were made without using the small angle assumptions or neglecting the influence of roll due to rudder deflection. The simplifying assumptions made in the analysis of the damper contributions were found to be justified.

ADVANTAGE OF YAW DAMPER STABILIZATION

It was pointed out in the Introduction that aerodynamic damping should be augmented by some other means than increasing the tail length or area. Increased tail length is limited by operational factors such as carrier elevator sizes for naval aircraft. The amount of vertical tail area also has a practical limitation which precludes the increases in damping that are desired.

The yaw damper has the advantage of increasing C_{n_r} without affecting the value of C_{n_β}. Tail size can then be chosen without consideration of the requirement of high damping, and C_{n_β} can be set from consideration of static stability, stalling qualities, etc. Dismissing the possibility of adding to conventional tail length, the vertical tail area would have to be increased by a factor of about four to achieve the same results in damping that the addition of this stabilizer will.

Reference 8 points out that with the XB-47 it was physically impossible to change the effective dihedral negatively enough to correct the lateral dynamics because of ground clearance, and that the tail area would have to be at least doubled to add the necessary damping. It was explained that in general, while increasing tail size increases damping, the gain in smooth flying qualities is questionable. While the tail size increase adds to the damping, the excitation of the aircraft due to side gusts increases in the same proportion.

This XB-47 report uses the servomechanisms approach to stability analysis as outlined in references 11 and 12. In one polar stability plot White shows that the effect of increasing C_{n_r} and C_{n_β} together (as in the

case of increasing tail area) results in little or no improvement in damping because the resonant frequency of the aircraft has been increased.

Consider the single degree of freedom equation in yaw,

$$I_z \ddot{\psi} - C_{n_{\dot{\psi}}} \dot{\psi} + C_{n_\beta} \psi = -C_{n_{\delta_r}} \delta_r$$

This equation may be transformed into the standard servomechanisms form using the following definitions:

damping ratio $$\zeta = \frac{-C_{n_{\dot{\psi}}}}{2 I_z \omega_o}$$

undamped natural frequency $$\omega_o^2 = \frac{C_{n_\beta}}{I_z}$$

rudder effectiveness $$K_\delta = \frac{C_{n_{\delta_r}}}{C_{n_\beta}}$$

The equation of motion then becomes

$$\ddot{\psi} + 2\zeta \omega_o \dot{\psi} + \omega_o^2 \psi = K_\delta \omega_o^2 \delta$$

and the

damped natural frequency $$\omega_n = \omega_o \sqrt{1 - \zeta^2}$$

resonant frequency $$\omega_r = \omega_o \sqrt{1 - 2\zeta^2}$$

For the usual values of ζ, ω_o, ω_r, and ω_n may be considered equal. White, reference 8, considering the single degree of freedom case, sets up his criterion of damping as the ratio of dynamic yaw response occurring at ω_r, to the effective static yaw response considering $\omega_r = \omega_o$.

The measure of the damping then becomes inversely proportional to the square of the undamped natural frequency, hence inversely proportional to C_{n_β}, since $\omega_r^2 \approx \omega_o^2 = C_{n_\beta}/I_z$.

Also from the single degree of freedom equation,

$$C_{1/2} = \frac{.693\sqrt{1-\zeta^2}}{2\pi\zeta}$$

White states that within the limits of engineering accuracy, the single degree of freedom equations may be used for calculations involving the design of the yaw damper and to obtain $C_{1/2}$.

Results from single degree of freedom calculations are included in Table III.

TRANSIENT RESPONSE INVESTIGATIONS

In order to graphically present the contrast between the transient response of the aircraft with and without the damper system operating, the following calculations were made. For condition II the responses ψ/β_o, β/β_o, and ϕ/β_o were found for a disturbance in sideslip effecting each of the three equations of motion. The function introduced is a unit step function in sideslip applied as a step function at $t = 0$, and neutralized as a step function at $t = 1$. Condition II was selected because in this configuration pilots have frequently reported unpleasant lateral oscillations. The forcing function used is an attempt to simulate a disturbance that might be initiated by turbulence or by a quick displacement in sideslip however introduced.

The airplane in the original condition is seen to have persistent oscillations in all three plots (figures 5, 6, and 7). The period is long enough so that the average pilot could damp them out with the proper application of controls; however, requiring the pilot to continually oppose these motions is tiring and detrimental to carrying out his mission. There is a considerable improvement in yawing velocity and sideslip, but the rolling characteristic with the damper in operation should be investigated in flight test. Too high a ratio of roll to sideslip is particularly unpleasant to the pilot. From data available in other applications, oscillations that damp to half amplitude in less than half a cycle appear dead beat to the pilot.

From this data and the rudder hinge moment parameters, the rudder pedal force that must be supplied by the servo power section of the damper can be estimated. An estimate of the amount of rudder throw required of the

damper rudder surface can also be made. The final setting of the stops limiting the throw of the damper rudder surface must be determined experimentally since the control required will depend upon the characteristics of the servo system as well as the airplane responses and the frequency range to be damped.

The response to an aileron step function is presented in figures 8, 9, and 10. Condition III is investigated since it is probably the most unfavorable. Adverse yaw has been included in the calculations. The large positive yaw due to roll introduced by the yaw damper is seen to drastically change the initial response upon entry into the rolling maneuver. The airplane no longer starts to yaw in the wrong direction for the turn, and the roll builds up rapidly. The sideslip builds up at a slightly faster rate also, but not rapidly enough to offset the good effects in yaw and roll. The derivative network in the yaw damper circuit will have an RC circuit with a time constant so designed as to only pass the first portion of a second of the contribution of the damper so that it will have the effect of assisting in the rapid build-up of roll without the adverse initial yaw, and still not oppose the steady-state maneuver. In this manner the damper should considerably improve the response to the rolling control.

From figure 5, (the response in yawing velocity to the disturbance in sideslip) the maximum yawing velocity per degree disturbance is seen to be approximately two degrees per second per degree sideslip. Then ten degrees of rudder would be required for a gain of one and an initial disturbance of five degrees, since $\delta_r = \left| d\delta_r / d\dot{\psi} \right| \dot{\psi}$.

Considering a ten degree throw in either direction as the limit for

damper applied rudder deflection, it can be seen that the "with damper" curves shown in the aileron response plots will be cut off by the rudder reaching its stops. This cut-off point will be determined by the amount of aileron applied since figure 9 is presented per degree deflection. When the product of the gain and the yawing velocity exceeds the available full deflection, the rudder will be initially held against the stop with a ten degree favorable deflection. The RC circuit will then cut out the damper rudder contribution as the steady signal is sensed by the gyro. Should there be a tendency to oscillate, the servomechanism will damp the variations about the steady maneuver out.

The curves showing the improved performance with the damper operating (figures 8, 9, and 10) will then be modified by servo rudder stop setting. Startling improvement in the entry into rolling maneuvers should still be obtainable with limited rudder throw.

Two factors should be here reiterated. First, these calculations were made for the maximum value of gyro axis inclination, and hence positive C_{n_p} increment, possible at the selected value of gain. In other words these aileron responses are for the maximum gearing of the rudder to the ailerons. Some smaller angle of gyro axis inclination might prove more desirable from flight test or more exhaustive calculations. Second, the device introduced to assure nearly constant contributions from the damper with variations in speed and altitude will automatically reduce the gain at higher velocities. This should prevent destructive rudder motions as it hits its stop after the gyro senses a large rolling velocity.

DETERMINATION OF CRITICAL TIME LAG

In all the calculations to this point the assumption has been made that the time lag of the damper system is zero. The critical time lag of the aircraft-autopilot combination is now investigated to determine how much of a limitation this assumption imposes.

The frequency response method outlined in reference 14 is applied. The critical time lag of the system is defined as the time lag that results in a neutrally stable or steady-state oscillation. The steady-state response $K_A = |\dot{\Psi}/\delta_n|$ of the airplane to a sinusoidal forcing function of unit amplitude was first calculated. The calculations were made for condition III since in this condition the ratio of the damping to the critical damping was lowest. The gain of the yaw damper is known, having been set at K=1 for this condition. The gain, K, is the amplitude of the control-surface oscillation produced by the yaw damper mechanism in response to the oscillation of the airplane yawing velocity. Intersecting $K_c = |1/K|$ with the airplane gain or amplitude plot the maximum permissible time lag in the system can be determined. The slope of the line through the point where the phase angles are equal is a measure of this critical time lag. The condition for stability is that at each angular frequency where the phase angles are equal, the ratio of the amplitudes of the airplane to the autopilot must be less than one.

From figure 11 the critical time lag of the system chosen is seen to be 1.2 seconds. Critical time lags for gains of two and three are shown also. For a damper gain of three, the limiting time lag is .7 considerably in excess of that inherent in typical force type systems. The critical lag

shown in reference 8 is a little over .5 seconds for $K = 1$. For servomechanisms with larger time lags introduced by boost systems, this calculation would undoubtedly show a closer margin. In this case, the time lag of the system is not a limiting consideration.

CONCLUSIONS

As a result of the theoretical investigation of the application of a yaw damping servomechanism to the aircraft under consideration, the following conclusions are reached:

(1) This plane does not satisfactorily meet the requirements of reference 1 in regard to lateral-directional oscillations. Control-fixed calculations predict that the airplane will exhibit a "Dutch Roll" in all the conditions investigated to a degree that could be classified as objectionable but not dangerous. These calculations substantiate pilots reports of "snaking" or "Dutch Roll."

(2) By installing the yaw damper system as proposed, the aircraft will then meet the requirements of reference 1. The lateral oscillations will appear nearly critically damped to the pilot, and he will be able to carry out the mission of the aircraft more effectively with less effort.

(3) The damper will introduce enough damping in yaw to make the aircraft always spirally stable. It will also introduce a constant positive yawing moment due to roll which will improve the turning and rolling performance. The system will be so designed as to improve entry into steady turning or rolling maneuvers, but not oppose them.

(4) Damping introduced by a servomechanism which applies rudder control proportional to yawing velocity is probably the most promising if not the only satisfactory way to augment the aerodynamic damping. This stabilizer introduces damping without increasing the resonant frequency (or the effective static yaw stability), which insures results not obtainable by increasing vertical tail area.

(5) For this particular installation the optimum settings of gyro spin axis angle and damper gain are $\Delta = 30^{\circ}$ and $K = 1$. These values have been checked in a limiting condition and the amount of positive yaw due to roll introduced is within the limit that would cause a long period unstable oscillation. Some lower value of Δ that would still produce a $+C_{n_{\dot{\phi}}}$ might prove more desirable from flight tests of the effect on rolling maneuvers. In all cases, the spin axis of the gyro should be kept below the stability or wind axis. Figure 1c.

(6) It should be required in the case of a stabilizing system (as opposed to an autopilot) that no feedback to the pilots controls be allowed. In this case the most practical solution appears to be the use of a separate rudder area for the yaw damper mechanism, probably splitting the two piece rudder between the pilot and the damper. A differential linkage or gearing, with the pilot and stabilizer as independent inputs with provision for balancing out the servo applied hinge moments could be developed.

(7) Calculations show that the damper system as proposed will improve the transient response to a disturbance in sideslip, and also improve the response to an aileron step function input.

(8) The critical time lag of the stabilizer-airplane system is considerably in excess of the maximum time lag to be expected of any servomechanism of the type proposed. The assumption of zero time lag in the calculations proved to be reasonable.

White, in reference 8, has an excellent presentation for the investigation of the stability of the stabilizer-airplane combination which he calls the inverse frequency response method. It is felt that this type of approach

should be used after the experimental frequency response data of the actual servomechanism to be used is available. Otherwise results would be of academic interest only. The method presented here will enable the designer to quickly select a system with the required gain, time lag, and power output from the servo drive and install it near the optimum position relative to the airplane reference axis. Flight testing the system from that point would probably yield the quickest dependable results unless an analog computer were available.

CALCULATIONS

The lateral equations of motion are given in reference 9. In all cases C_{Y_p}, C_{Y_r}, and γ were assumed to be zero. The equations including the product of inertia were used only in case I. Otherwise they were used as follows:

$$(m_o D - C_{Y_\beta})\beta - C_L \phi + m_o D \Psi = 0$$

$$-C_{\ell_\beta}\beta + (I_x D^2 - C_{\ell_{\dot{\phi}}} D)\phi - C_{\ell_{\dot{\psi}}} D\Psi = 0$$

$$-C_{n_\beta}\beta - C_{n_{\dot{\phi}}} D\phi + (I_z D - C_{n_{\dot{\psi}}})D\Psi = 0$$

then,

$$b_4 \lambda^4 + b_3 \lambda^3 + b_2 \lambda^2 + b_1 \lambda + b_o = \Delta = 0$$

where

$$b_4 = m_o I_x I_z$$

$$b_3 = -(m_o C_{\ell_{\dot{\phi}}} + C_{Y_\beta} I_x) I_z - m_o I_x C_{n_{\dot{\psi}}}$$

$$b_2 = C_{Y_\beta} C_{\ell_{\dot{\phi}}} I_z + (m_o C_{\ell_{\dot{\phi}}} + C_{Y_\beta} I_x) C_{n_{\dot{\psi}}} + m_o I_x C_{n_\beta} - m_o C_{\ell_{\dot{\psi}}} C_{n_{\dot{\phi}}}$$

$$b_1 = -C_{Y_\beta} C_{\ell_{\dot{\phi}}} C_{n_{\dot{\psi}}} + m_o C_{\ell_\beta} C_{n_{\dot{\phi}}} - m_o C_{\ell_{\dot{\phi}}} C_{n_\beta} - C_L C_{\ell_\beta} I_z + C_{Y_\beta} C_{\ell_{\dot{\psi}}} C_{n_{\dot{\phi}}}$$

$$b_o = C_L (C_{\ell_\beta} C_{n_{\dot{\psi}}} - C_{\ell_{\dot{\psi}}} C_{n_\beta})$$

The fastest and most accurate method for the solution of the stability quartic was to use a combination of the Lin approximation method and the Zimmerman plot as explained in references 11 and 13. With the Lin method, values could be obtained that would lead to an intersection in two or three points with the Zimmerman plot. In general, there were two real roots and a

complex pair, although where a large value of $+C_{n_{\dot{\phi}}}$ was used there were two complex pairs.

Where the roots were λ_1, λ_2 and $\alpha \mp i\beta$,

$$T_{1/2} = \frac{.693}{\alpha} \text{ seconds}$$

$$P = \frac{2\pi}{\beta} \text{ seconds}$$

$$C_{1/2} = .1102 \frac{\beta}{\alpha}$$

For the plots in figures 3 and 4, where each point represents the solution of a quartic, the equations for $b_{4,3,2,1,0}$ were used where the variables were $C_{n_{\dot{\phi}}}$ and $C_{n_{\dot{\psi}}}$ determined from the particular value of $\zeta = \zeta(\alpha,\omega)$ for that point.

Using the above three equations of motion, a general solution for forcing function inputs of A. B. and C respectively was made. The transient responses took the following forms:

$$\frac{\dot{\psi}}{\delta(t)} = \frac{a_3\lambda^3 + a_2\lambda^2 + a_1\lambda + a_o}{\Delta}$$

where

$$a_3 = Cm_oI_x$$

$$a_2 = AC_{n_\beta}I_x + Bm_oC_{n_{\dot{\phi}}} - C(m_oC_{\ell_{\dot{\phi}}} + C_{Y_p}I_x)$$

$$a_1 = A(C_{\ell_\beta}C_{n_{\dot{\phi}}} - C_{n_\beta}C_{\ell_{\dot{\phi}}}) - BC_{n_{\dot{\phi}}}C_{Y_\beta} + CC_{\ell_{\dot{\phi}}}C_{Y_\beta}$$

$$a_o = BC_LC_{n_\beta} - CC_LC_{\ell_\beta}$$

$$\frac{\beta}{\delta(t)} = \frac{a_3\lambda^3 + a_2\lambda^2 + a_1\lambda + a_o}{\Delta}$$

where

$$a_3 = AI_xI_z$$

$$a_2 = -A(I_xC_{n_{\dot{\psi}}} + I_zC_{\ell_{\dot{\phi}}}) - Cm_oI_x$$

$$a_1 = A(C_{\ell_{\dot{\phi}}}C_{n_{\dot{\psi}}} - C_{n_{\dot{\phi}}}C_{\ell_{\dot{\psi}}}) + B(C_LI_x - m_oC_{n_{\dot{\phi}}}) + Cm_oC_{\ell_{\dot{\phi}}}$$

$$a_o = -BC_LC_{n_{\dot{\psi}}} + CC_LC_{\ell_{\dot{\psi}}}$$

$$\frac{\phi}{\delta(t)} = \frac{a_2\lambda^2 + a_1\lambda + a_o}{\Delta}$$

where

$$a_2 = Bm_oI_z$$

$$a_1 = AC_{\ell_\beta}I_z - B(m_oC_{n_{\dot{\psi}}} + I_zC_{Y_\beta}) + Cm_oC_{\ell_{\dot{\psi}}}$$

$$a_o = -A(C_{\ell_\beta}C_{n_{\dot{\psi}}} - C_{n_\beta}C_{\ell_{\dot{\psi}}}) + B(C_{Y_\beta}C_{n_{\dot{\psi}}} + m_oC_{n_\beta}) - C(m_oC_{\ell_\beta} + C_{Y_\beta}C_{\ell_{\dot{\psi}}})$$

In the solution for the disturbance in β, $\delta(t)$ became β_o, and A, B, and C were C_{Y_β}, C_{ℓ_β}, and C_{n_β}.

In the response to the aileron step function, $\delta(t)$ became δ_a and A, B, and C were 0, $C_{\ell_{\delta_a}}$, and $C_{n_{\delta_a}}$.

Δ, and hence the roots λ_1, λ_2, and $\alpha \mp i\beta$ are known.

The solution for the typical lateral transient response takes the form

$$g(t) = C_o + C_1\ell^{\lambda_1 t} + C_2\ell^{\lambda_2 t} + E\ell^{\alpha t}\sin(\beta t + F)$$

By use of the Heaviside Expansion Theorem,

$$C_o = \frac{a_o}{b_o}$$

$$C_r = \frac{a_3\lambda_r^3 + a_2\lambda_r^2 + a_1\lambda_r + a_o}{\lambda_r(4b_4\lambda_r^3 + 3b_3\lambda_r^2 + 2b_2\lambda_r + b_1)}$$

Then from end conditions

$$E = \frac{-(C_o + C_1 + C_2)}{\sin F}$$

$$\tan F = \frac{-\beta(C_o + C_1 + C_2)}{C_3 - \lambda_1 C_1 - \lambda_2 C_2 + \alpha(C_o + C_1 + C_2)}$$

where C_3 represents the initial condition of $\dot{\psi}$, $\dot{\beta}$, or $\dot{\phi}$ at $t = 0$. $C_3 = \frac{a_3}{b_4}$. An initially relaxed system is assumed.

To find the frequency response for the critical time lag calculations, standard servomechanisms methods were used. It is believed that the best method of reducing the data is outlined in reference 8, and is as follows:

For the airplane,

$$\frac{\dot{\psi}}{\delta_r} = \frac{a_3D^3 + a_2D^2 + a_1D + a_o}{b_4D^4 + b_3D^3 + b_2D^2 + b_1D + b_o}$$

Using the general equations developed previously with forcing functions A, B, and C as $C_{Y_{\delta_r}} \sin \omega t$, $C_{\ell_{\delta_r}} \sin \omega t$, and $C_{n_{\delta_r}} \sin \omega t$ the a's can be quickly calculated.

Then K_A , the steady-state frequency response of the airplane, can

be expressed

$$K_A = \frac{\dot{\psi}}{\delta_r} = \frac{X_1 + iY_1}{X_2 + iY_2} = \left|\frac{\dot{\psi}}{\delta_r}\right| e^{i(\phi_1 - \phi_2)}$$

where the substitution $D = i\omega$ is made.

$$X_1 = -a_2\omega^2 + a_o \qquad X_2 = \omega^4 - b_2\omega^2 + b_o$$

$$Y_1 = -a_3\omega^3 + a_1\omega \qquad Y_2 = -b_3\omega^3 + b_1\omega$$

$$\phi_1 = \tan^{-1}\frac{Y_1}{X_1} \qquad \phi_2 = \tan^{-1}\frac{Y_2}{X_2}$$

Then for each frequency the magnitude of the airplane gain or amplitude is

$$|K_A| = \left|\frac{\dot{\psi}}{\delta_r}\right| = \frac{X_1 \cos\phi_2}{X_2 \cos\phi_1}$$

and the phase angle is

$$\phi = \phi_1 - \phi_2$$

REFERENCES

1. Anon.: Specification for Flying Qualities of Piloted Airplanes. NAVAER SR-119B, BuAir, 1 June 1948.

2. Stough, C.J., and Kauffman, W.M.: A Flight Investigation and Analysis of the Lateral Oscillation Characteristics of an Airplane. NACA TN 2195. 1950.

3. Schy, A.A.: A Theoretical Analysis of the Effects of Fuel Motion on Airplane Dynamics. NACA TN 2280. 1951.

4. Sternfield, Leonard,: Some Effects of Non-Linear Variation in the Directional Stability and Damping-in-Yawing Derivatives on the Lateral Stability of an Airplane. NACA TN 2233. 1950.

5. Sternfield, Leonard,: Effect of Product of Inertia on Lateral Stability. NACA TN 1193. 1947.

6. Anon.: Lear Aircraft Damper System, N-834, Leqr Incorporated.

7. Sternfield, Leonard.: Effect of Automatic Stabilization on the Lateral Oscillatory Stability of a Hypothetical Airplane at Supersonic Speeds. NACA TN 1818. 1949.

8. White, R.J.: Investigation of Lateral Dynamic Stability in the XB-47 Airplane. Published by IAS.

9. Sternfield, Leonard.: Some Considerations of the Lateral Stability of High Speed Aircraft. NACA TN 1282. 1947.

10. Johnson, J.L., and Sternfield, L.: A Theoretical Investigation of the Effect of Yawing Moment Due to Rolling on Lateral Oscillatory Stability, NACA TN 1723. 1948.

11. Brown, G.S. and Campbell, D.P.: Principles of Servomechanisms, John Wiley and Sons, Inc., New York. 1949.

12. Jones, A.L. and Briggs, B.R.: A Survey of Stability Analysis Techniques for Automatically Controlled Aircraft. NACA TN 2275. 1951.

13. Perkins, C.D. and Hage, R.E.: Airplane Performance Stability and Control, John Wiley and Sons, Inc., New York. 1950.

14. Sternfield, L. and Gates, O.B.: A Theoretical Analysis of the Effect of Time Lag in an Automatic Stabilization System on the Lateral Oscillatory Stability of an Airplane. NACA TN 2005. 1950.

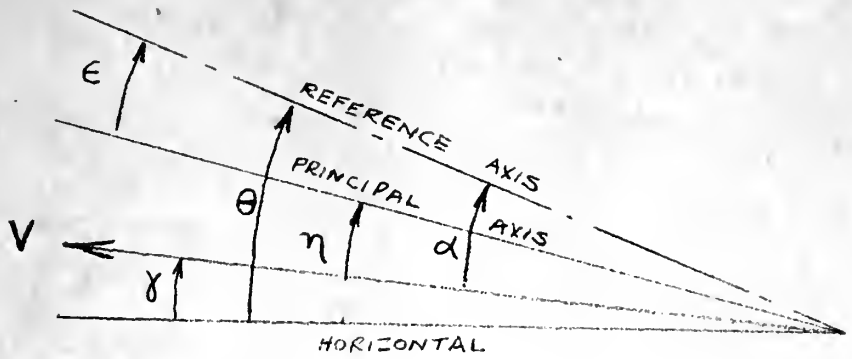

FIGURE 1a

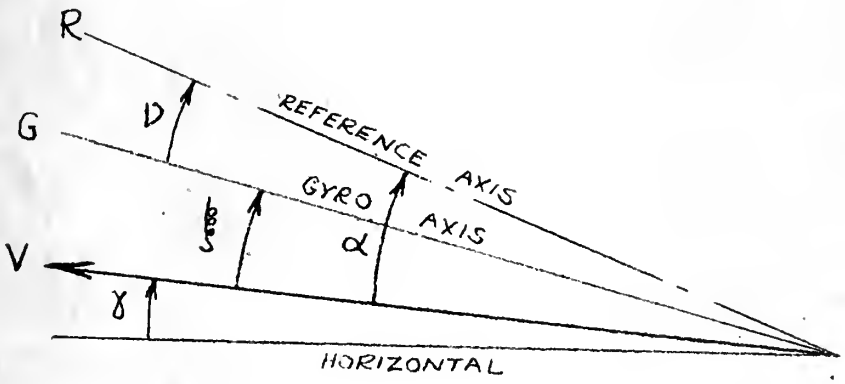

FIGURE 1b

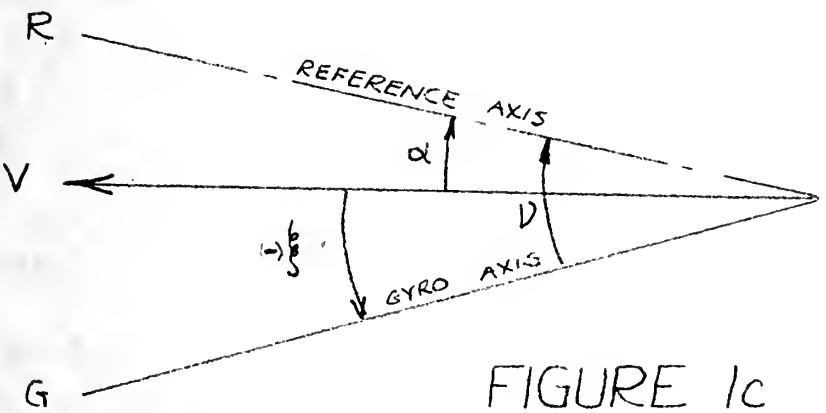

FIGURE 1c

POSITIVE DIRECTIONS INDICATED BY ARROWS

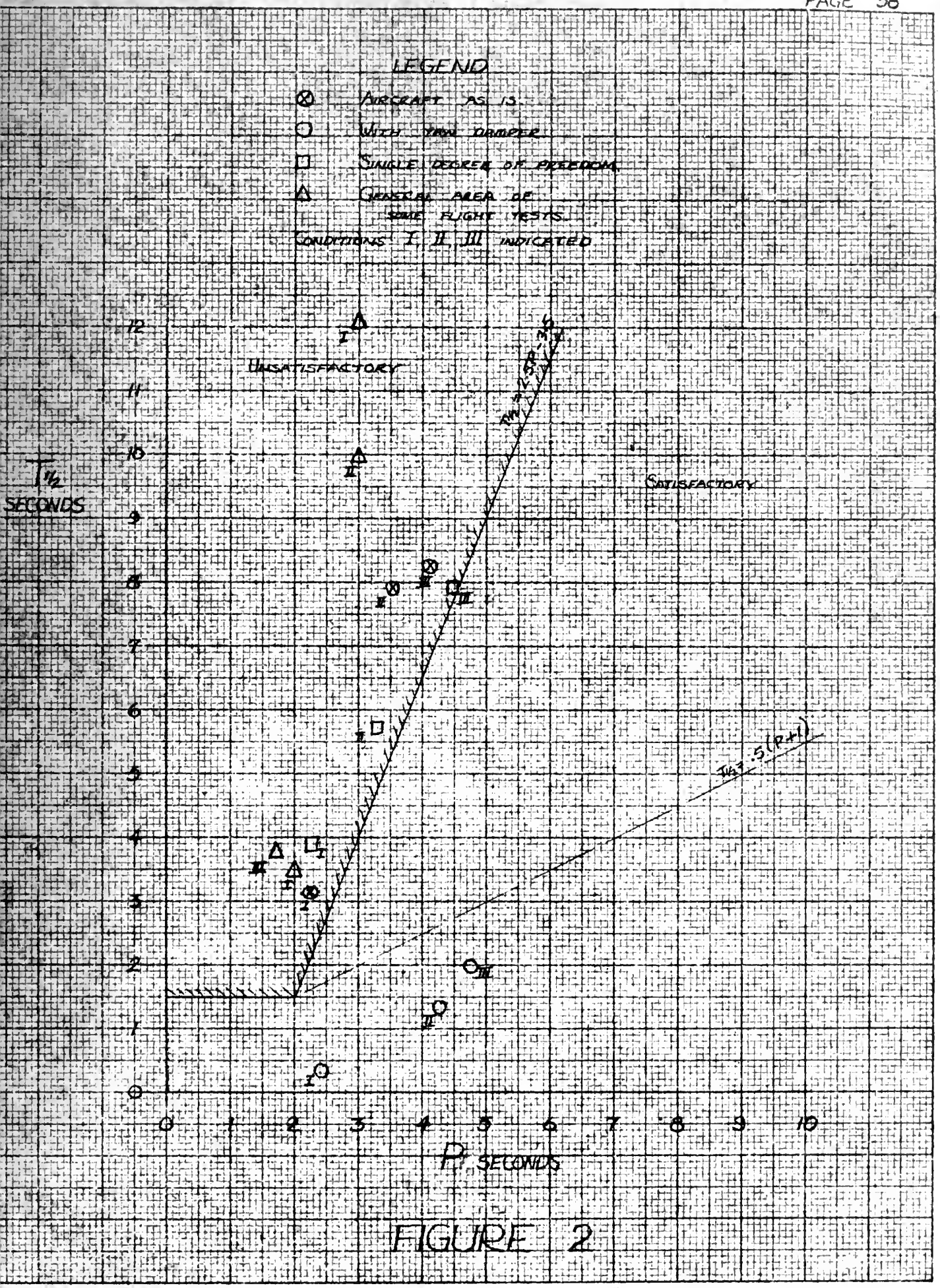
LEGEND
Aircraft as is
With yaw damper
Single degree of freedom
General area of some flight tests.
Conditions I, II, III indicated
Unsatisfactory
Satisfactory
$T_{1/2}$ SECONDS
P, SECONDS
$T_{1/2} = .5(P+1)$
0
1
2
3
4
5
6
7
8
9
10
11
12

FIGURE 2

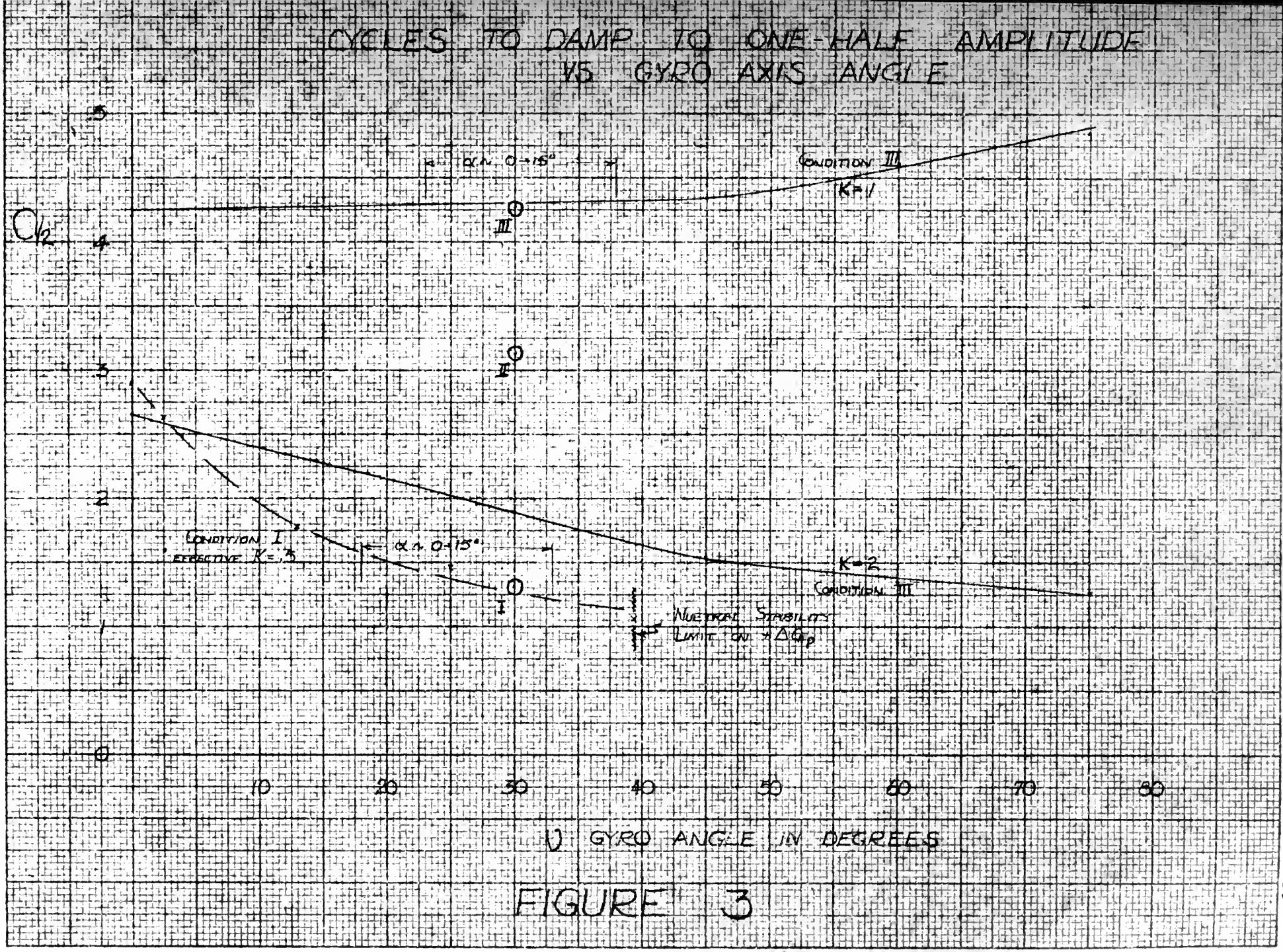
CYCLES TO DAMP TO ONE-HALF AMPLITUDE
VS GYRO AXIS ANGLE
$C_{1/2}$
5
4
3
2
1
0
10
20
30
40
50
60
70
80
α GYRO ANGLE IN DEGREES
α ∿ 0→15°
CONDITION III
K=1
III
II
I
CONDITION I
EFFECTIVE K=.5
α ∿ 0→15°
K=2
CONDITION III
NEUTRAL STABILITY
LIMIT ON $\pm\Delta\alpha_p$

FIGURE 3

CURVES AT CONSTANT GAIN VARYING GYRO ANGLE

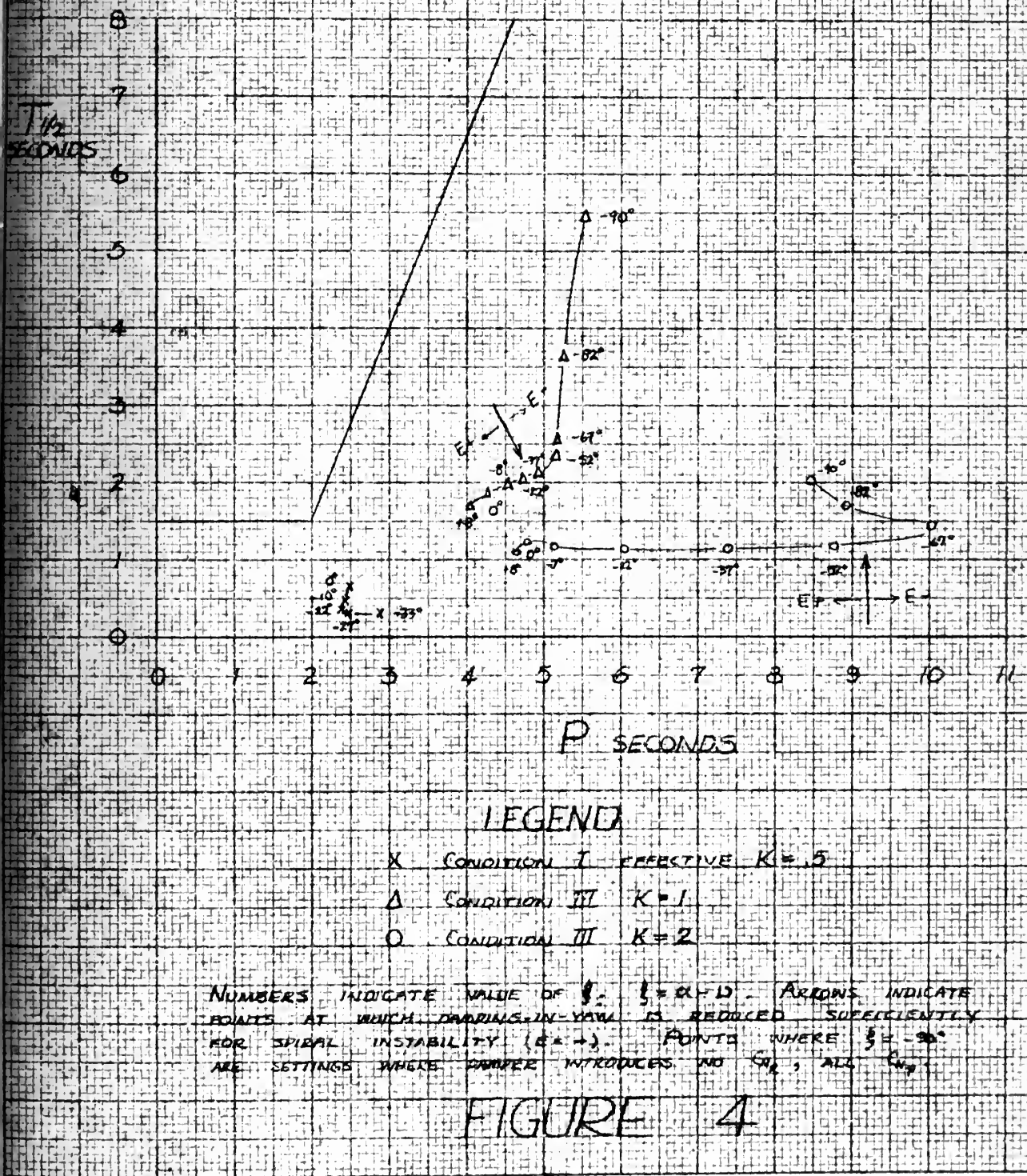

LEGEND

X Condition I effective K = .5

Δ Condition III K = 1

O Condition III K = 2

Numbers indicate value of ζ. $\zeta = \alpha - D$. Arrows indicate points at which damping-in-yaw is reduced sufficiently for spiral instability ($c = -$). Points where $\zeta = -90°$ are settings where damper introduces no C_{n_β}, all C_{n_p}.

FIGURE 4

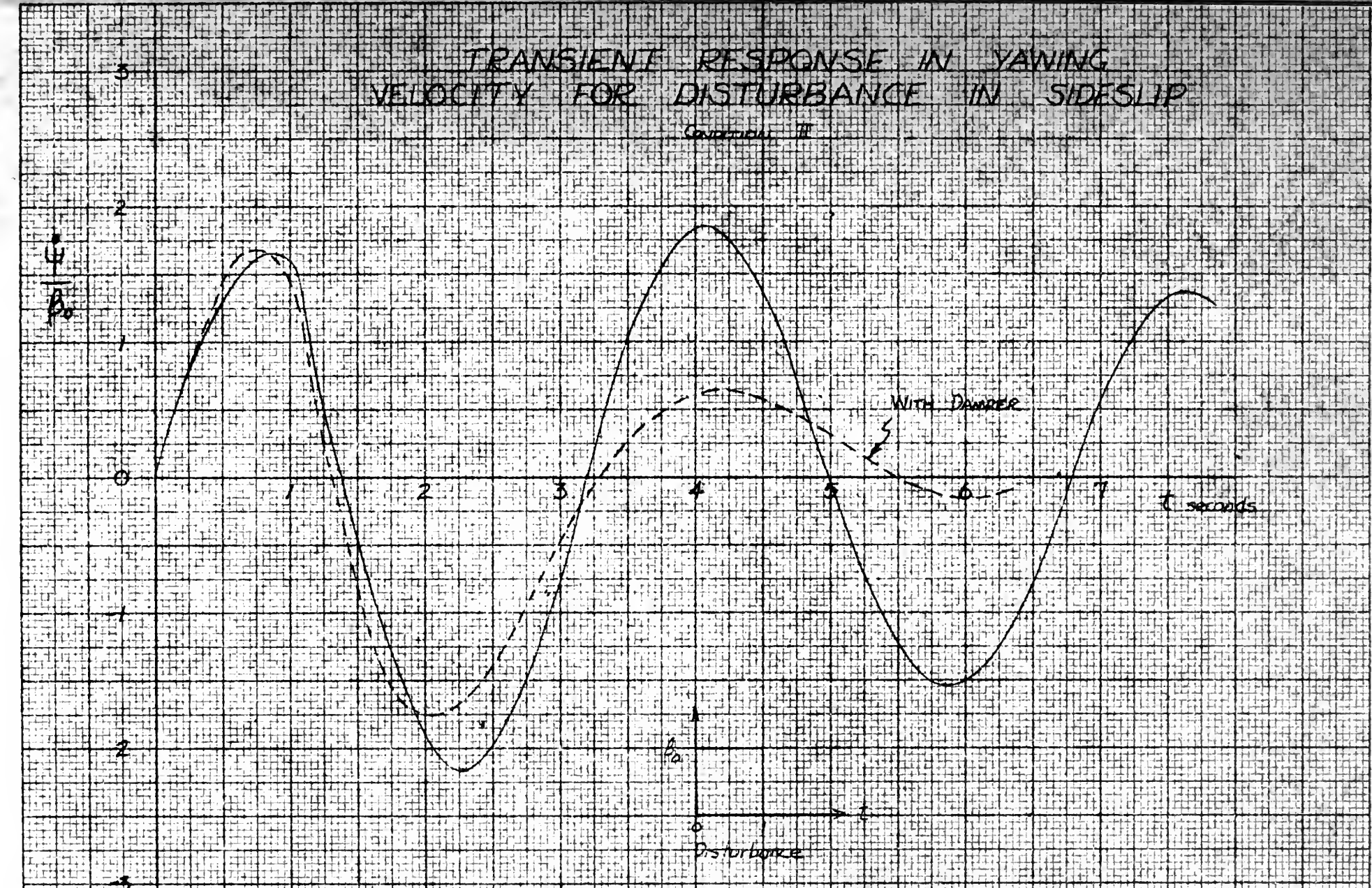
TRANSIENT RESPONSE IN YAWING VELOCITY FOR DISTURBANCE IN SIDESLIP
CONDITION II
$\frac{\dot{\psi}}{\beta_0}$
WITH DAMPER
t seconds
β_0
t
0
Disturbance

FIGURE 5

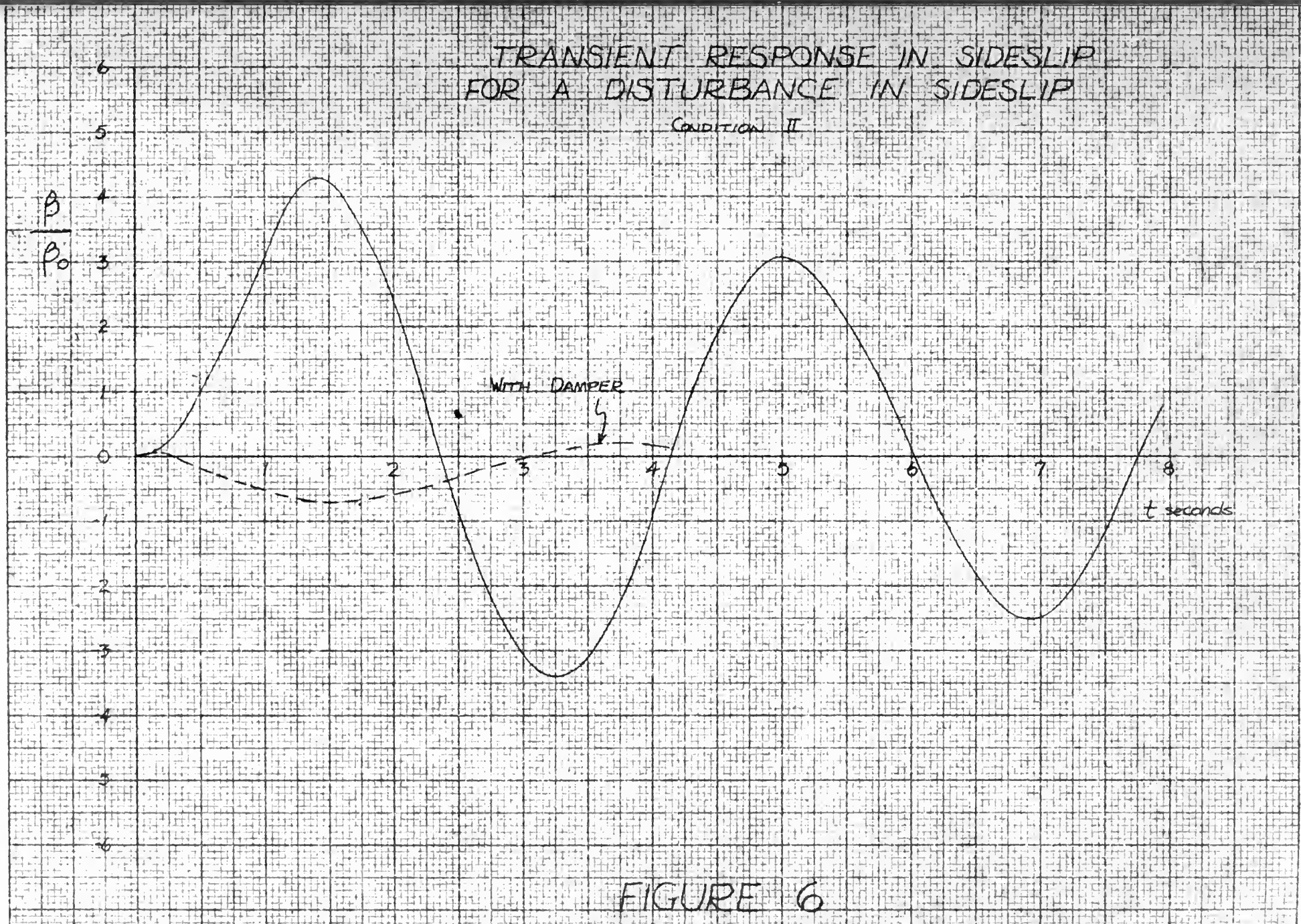
TRANSIENT RESPONSE IN SIDESLIP
FOR A DISTURBANCE IN SIDESLIP
CONDITION II
β/β₀
WITH DAMPER
t seconds
6
5
4
3
2
1
0
1
2
3
4
5
6
7
8

FIGURE 6

TRANSIENT RESPONSE IN ANGLE OF BANK FOR DISTURBANCE IN SIDESLIP

CONDITION II

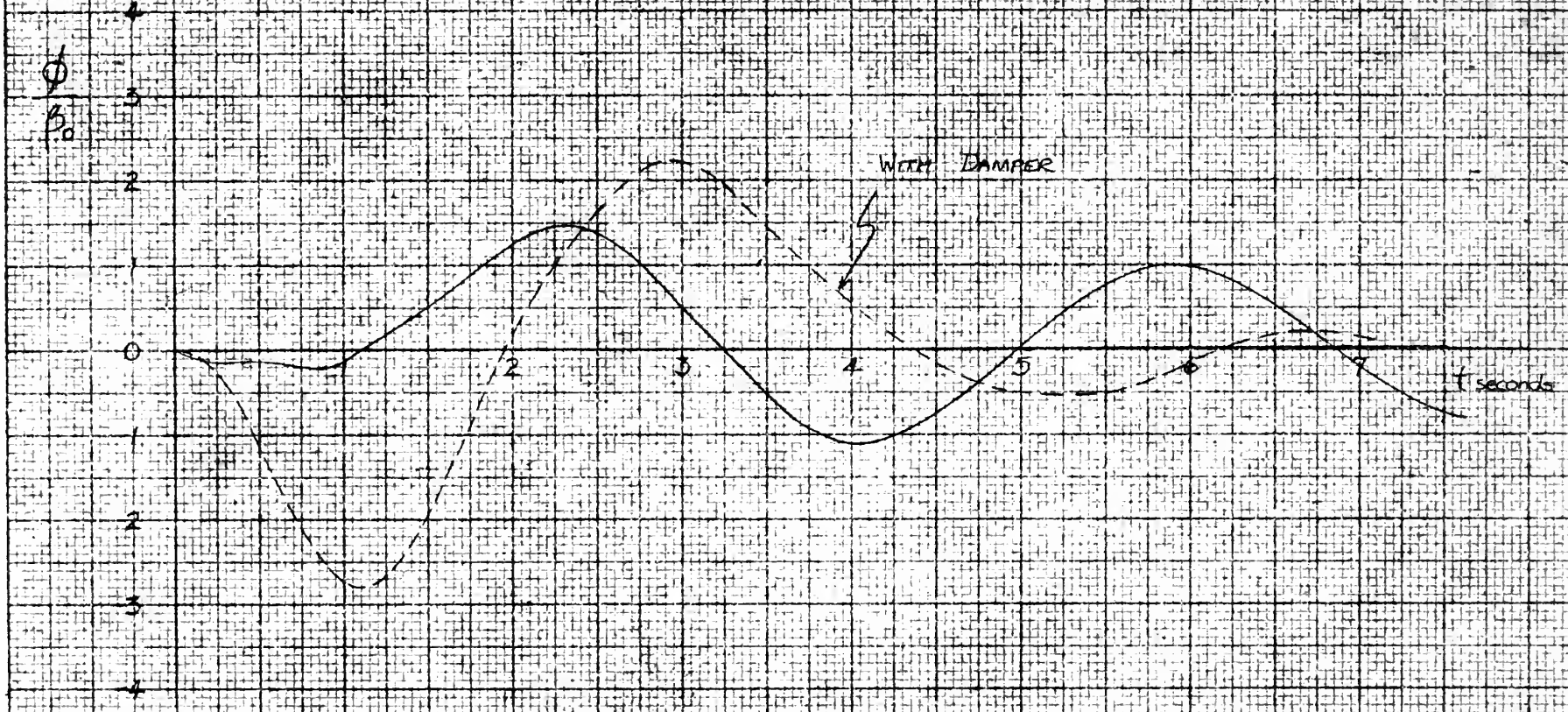

FIGURE 7

RESPONSE TO AILERON STEP-FUNCTION IN ANGLE OF BANK

CONDITION II

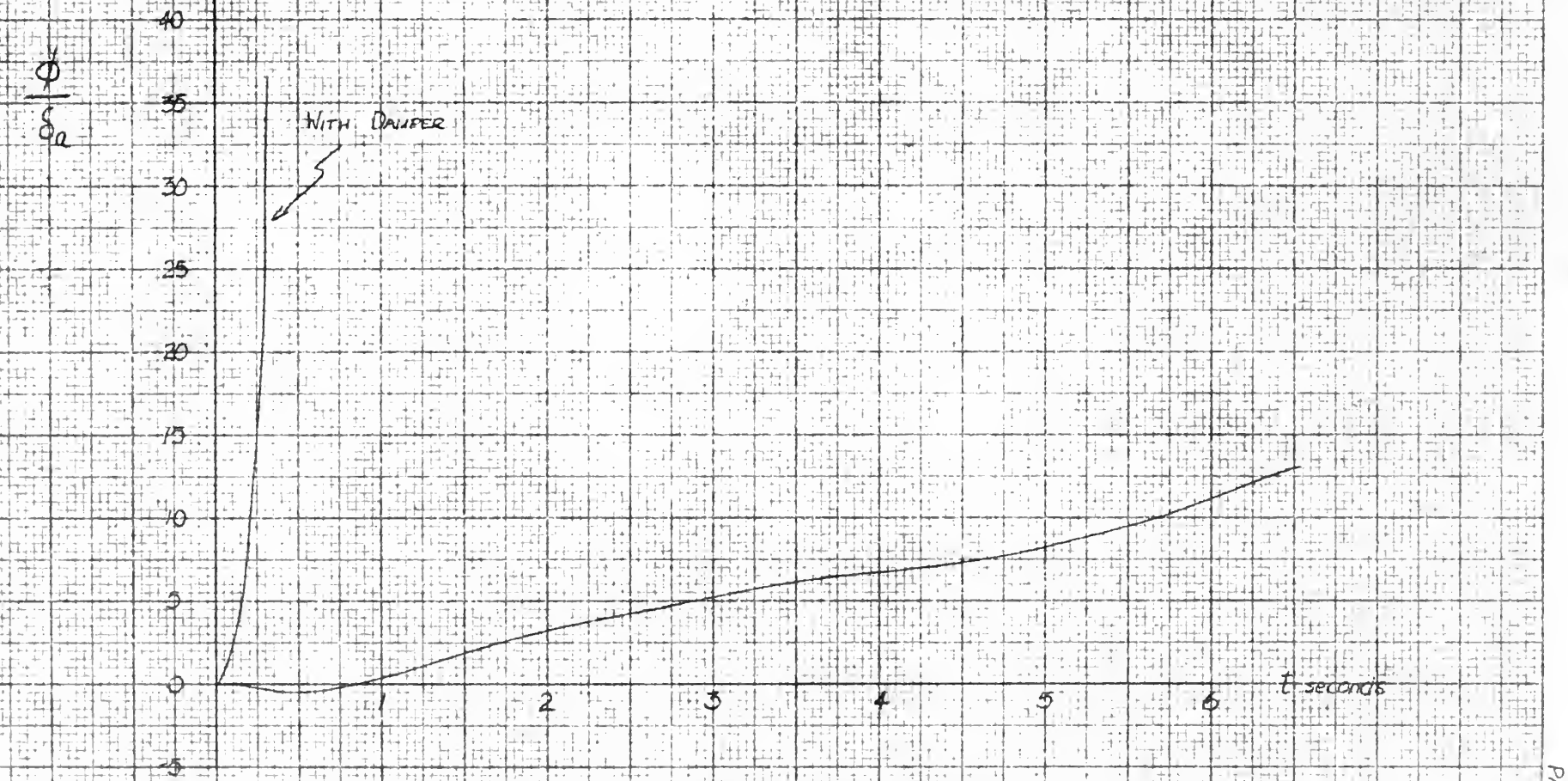

FIGURE 8

RESPONSE TO AILERON STEP-FUNCTION IN YAWING VELOCITY

CONDITION III

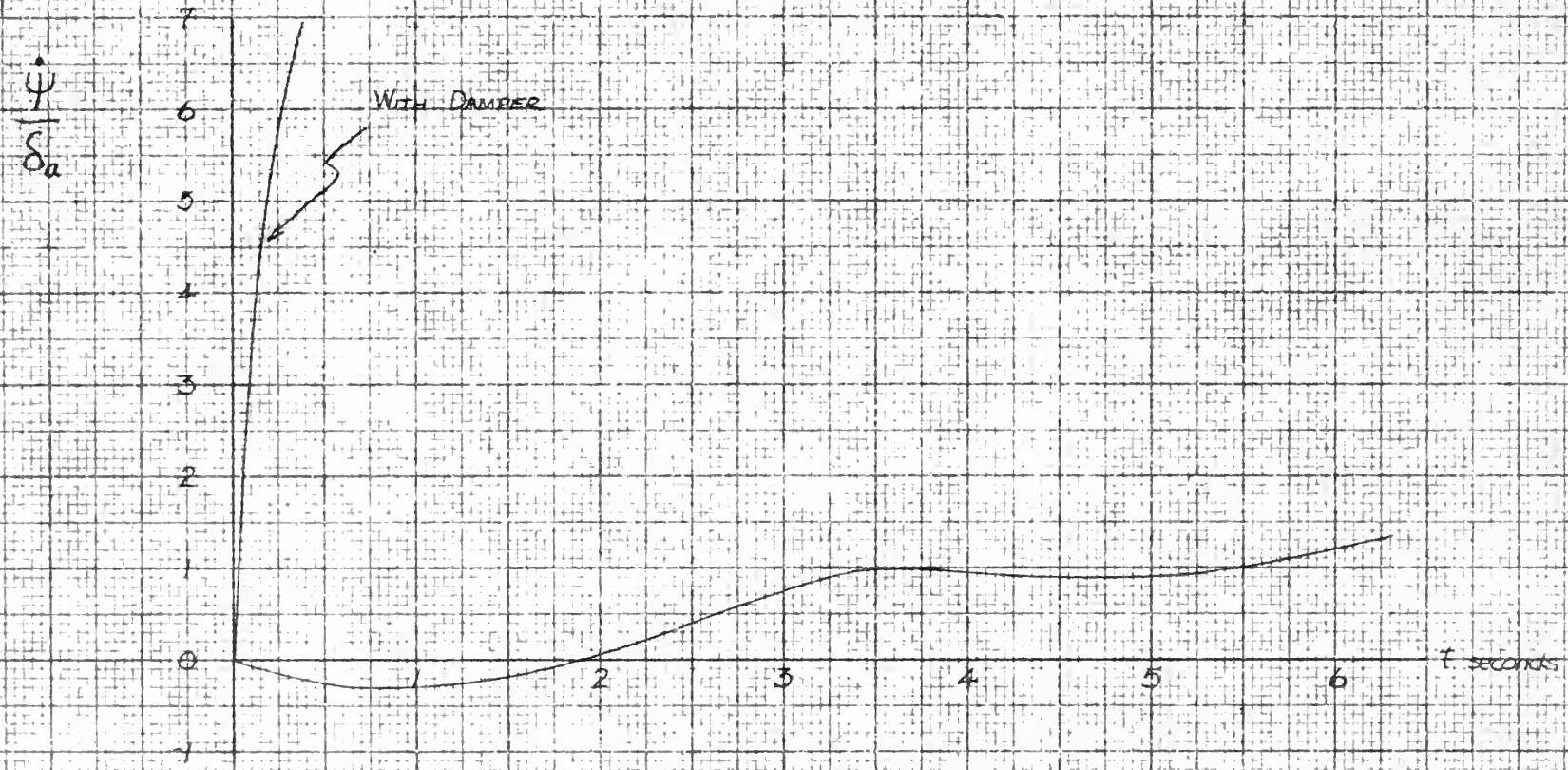

FIGURE 9

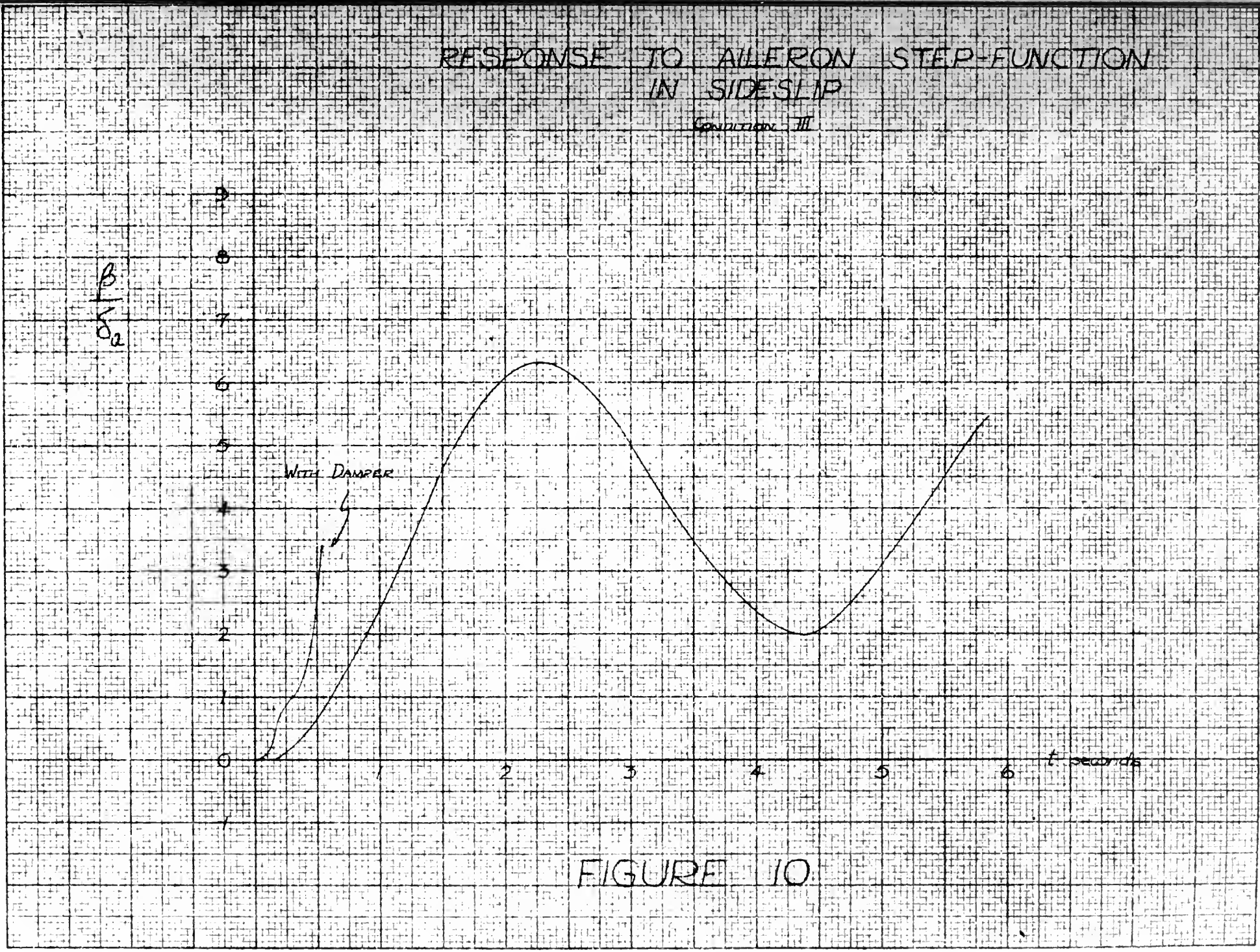
RESPONSE TO AILERON STEP-FUNCTION IN SIDESLIP
CONDITION III
$\frac{\beta}{\delta_a}$
9
8
7
6
5
4
3
2
1
0
1
2
3
4
5
6
t seconds
WITH DAMPER

FIGURE 10

DETERMINATION OF CRITICAL TIME LAG

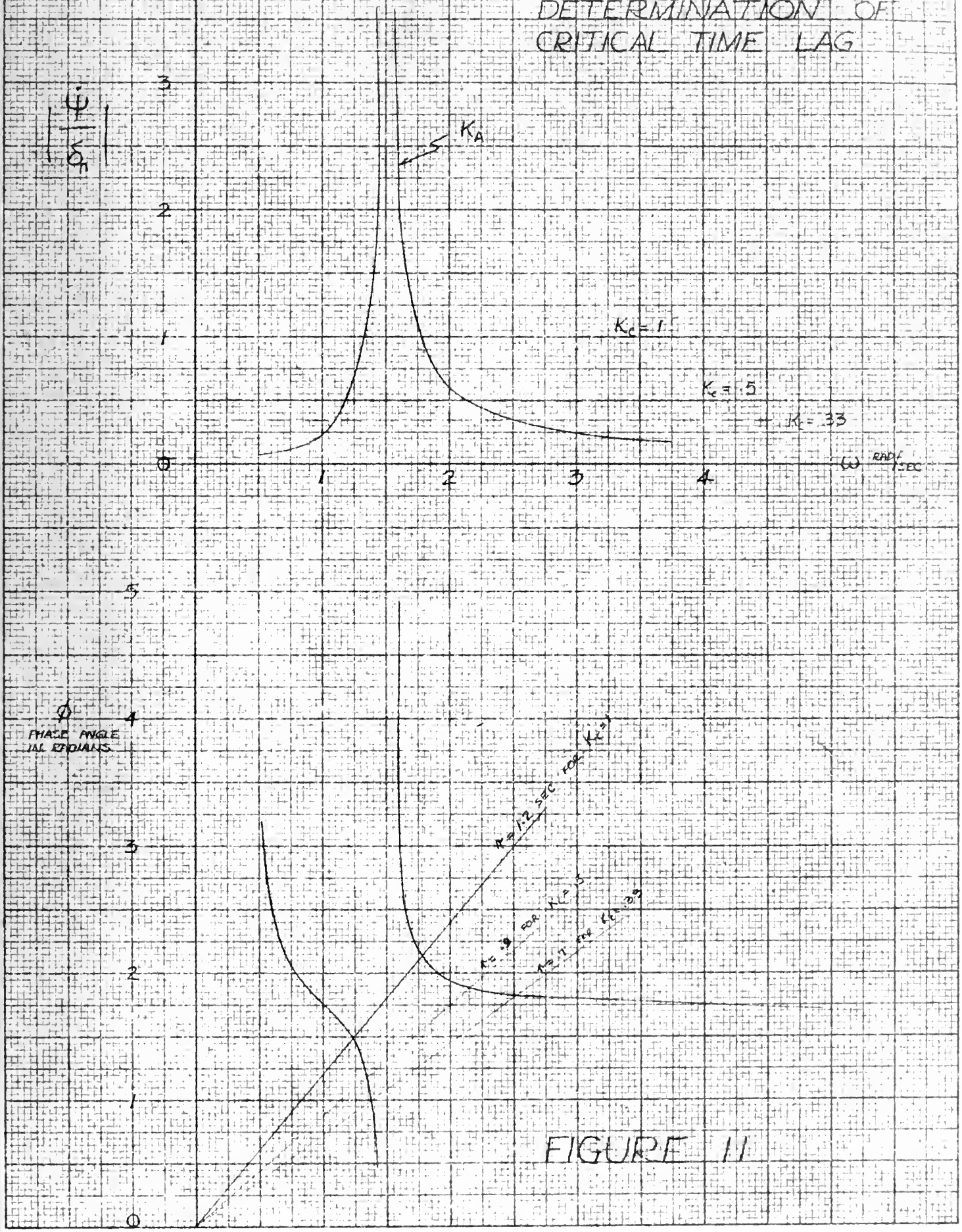

FIGURE 11

TABLE I

Principal Dimensions

S = 250 sq. ft.

b = 35.25 ft.

c_w = 7.45 ft.

l_t = 18.45 ft.

S_{vt} = 36 sq.ft.

S_r = 8.54 sq. ft.

c_{vt} = 6.75 ft.

b_{vt} = 7.42 sq. ft.

W = 12,000 pounds plus fuel

Total control throw for the rudder, $25^\circ \pm 1^\circ$ each way.

TABLE II

	Condition I	Condition II	Condition III
	CR max clean	50% NRP clean	Landing
h	35,000	10,000	sea level
V	660	259	183
M	.679	.323	.134
ρ	$.736(10)^{-3}$	$1.756(10)^{-3}$	$2.378(10)^{-3}$
W	13,500	13,500	12,500
μ	64.6	27.1	20.0
q	160.5	59.2	40.0
m_o	6.8	7.38	7.71
b/2V	.0267	.0681	.0964
C_L	.337	1.18	1.20
α	2.9	8.7	7.8
ϵ	3.63	3.63	4.07
η	-.73	5.07	3.73
D	30	30	30
δ_e	-27.1	-21.3	-22.2
I_{X_o}	7778	7778	7822
I_{Z_o}	24244	24244	24921
I_X	.0055	.0149	.0220
I_Z	.0172	.0465	.0688
I_{XZ}	.00015	-.0028	-.0030
K	.5	.817	1.0
C_{l_p}	-.546	-.400	-.400
C_{l_r}	.132	.174	.231
C_{l_β}	-.119	-.100	-.064

TABLE II (continued)

$C_{l_{\delta_r}}$	.0103	.0043	.0023
$C_{l_{\delta_a}}$			.082
$C_{l_{\dot{\phi}}}$	− .0146	− .0272	− .0386
$C_{l_{\dot{\psi}}}$	.0035	.0119	.0223
C_{n_p}	+ .0380	− .0350	− .0520
C_{n_r}	− .230	− .175	− .125
C_{n_β}	.135	.128	.135
$C_{n_{\delta_r}}$	− .0573	− .0444	− .0410
$C_{n_{\delta_a}}$			.015
$C_{n_{\dot{\psi}}}$	− .0062	− .0119	− .0121
$C_{n_{\dot{\phi}}}$	.0010	− .0024	− .0050
C_{Y_β}	− .671	− .562	− .344
$C_{Y_{\delta_r}}$			.115
P	2.26	3.56	4.13
$T_{1/2}$	3.15	7.93	8.28
$C_{1/2}$	1.26	1.94	2.05
T_2	spirally stable	31.5	15.1

With Yaw Damper Operative

$\Delta C_{n_{\dot{\psi}}}$	− .0255	− .0341	− .0379
$\Delta C_{n_{\dot{\phi}}}$	.0137	.0129	.0155
$C_{n_{\dot{\psi}}}$	− .0315	− .0450	− .0500
$C_{n_{\dot{\phi}}}$	.0147	.0115	.0105
P	2.44	4.28	4.73
$T_{1/2}$	.323	1. 35	2.02
$C_{1/2}$	.13	.31	.43

TABLE III

Single Degree of Freedom

	Condition I	Condition II	Condition III
I_Z	.0172	.0465	.0688
$C_{n\dot{\psi}}$	-.0061	-.0119	-.0121
C_{n_β}	.135	.128	.135
ω_o	2.805	1.661	1.404
ω_n	2.80	1.658	1.40
φ	.064	.077	.063
P	2.24	3.78	4.48
$T_{1/2}$	3.88	5.66	7.90
$C_{1/2}$	1.72	1.43	1.76
K for $C_{1/2}$ = .5	.26	.51	.76
$C_{1/2}$ if K = 1	.13	.304	.402

Thesis 16267
R39 Richardson
A theoretical analysis of the application of a yaw damper servomechanism to improve lateral oscillatory stability